








BRIEF COMMUNICATION

L1CAM variants cause two distinct imaging phenotypes on fetal MRI

Andrea Accogli^{1,2} , Stacy Goergen³, Giana Izzo⁴ , Kshitij Mankad⁵, Karina Kraijden Haratz⁶, Cecilia Parazzini⁴, Michael Fahey⁷, Lara Menzies⁸, Julia Baptista^{9,10} , Lucia Carpineta¹¹, Domenico Tortora¹² , Ezio Fulcheri^{13,14}, Valerio Gaetano Vellone¹⁴, Dario Paladini¹⁵, Luigina Spaccini¹⁶, Valentina Toto¹⁷, Claire Trayers¹⁸, Liat Ben Sira¹⁹, Adi Reches²⁰, Gustavo Malinger⁶, Vincenzo Salpietro^{2,21}, Patrizia De Marco¹, Myriam Srour²², Federico Zara^{1,2}, Valeria Capra¹ , Andrea Rossi^{12,23}  & Mariasavina Severino¹² 

¹Medical Genetics Unit, IRCCS Istituto Giannina Gaslini, Genoa, Italy

²Department of Neurosciences, Rehabilitation, Ophthalmology, Genetics, Maternal and Child Health, University of Genoa, Genoa, Italy

³Monash Imaging, Monash Health, Clayton, Victoria, Australia

⁴Department of Pediatric Radiology and Neuroradiology, V. Buzzi Children's Hospital, Milan, Italy

⁵Neuroradiology Unit, Great Ormond Street Hospital for Children, London, UK

⁶Division of Ultrasound in ObGyn, Lis Maternity Hospital, Tel Aviv Sourasky Medical Center, Affiliated to the Sackler Faculty of Medicine, Tel Aviv University, Tel Aviv, Israel

⁷Paediatric Neurology and Neurogenetics Units, Monash Children's Hospital Clayton, Clayton, Victoria, Australia

⁸Department of Clinical Genetics, Great Ormond Street Hospital, London, UK

⁹Exeter Genomics Laboratory, Royal Devon and Exeter NHS Hospital, Exeter, UK

¹⁰College of Medicine and Health, University of Exeter, Exeter, UK

¹¹Department of Pediatric Medical Imaging, Montreal Children's Hospital, McGill University, Montreal, Quebec, Canada

¹²Neuroradiology Unit, IRCCS Istituto Giannina Gaslini, Genoa, Italy

¹³Fetal-Perinatal Pathology Unit, IRCCS Istituto Giannina Gaslini, Genoa, Italy

¹⁴Department of Surgical Sciences and Integrated Diagnostics, Università di Genova, Genoa, Italy

¹⁵Fetal Medicine and Surgery Unit, IRCCS Istituto Giannina Gaslini, Genoa, Italy

¹⁶Clinical Genetics Unit, Department of Obstetrics and Gynecology, V. Buzzi Children's Hospital, Milan, Italy

¹⁷Pathology Division, Department of Health Sciences, San Paolo Hospital, University of Milan, Milan, Italy

¹⁸Department of Paediatric Pathology, Addenbrooke's Hospital, Cambridge, UK

¹⁹Pediatric Radiology, Dana Children's Hospital, Tel Aviv Sourasky Medical Center, Affiliated to the Sackler Faculty of Medicine, Tel Aviv University, Tel Aviv, Israel

²⁰Wolfe PGD- Stem Cell Lab, Racine IVF Unit Lis Maternity Hospital, Tel Aviv Sourasky Medical Center, Affiliated to the Sackler Faculty of Medicine, Tel Aviv University, Tel Aviv Israel, Genetic Institute, Tel Aviv Sourasky Medical Center, Tel Aviv, Israel

²¹Pediatric Neurology and Muscular Diseases Unit, IRCCS Giannina Gaslini Institute, Genoa, Italy

²²Department of Pediatrics, Montreal Children's Hospital, McGill University Health Center (MUHC), Montreal, Canada

²³Department of Health Sciences DISSAL, University of Genoa, Genoa, Italy

Correspondence

Andrea Rossi, Neuroradiology Unit, IRCCS Istituto Giannina Gaslini, Via Gaslini 5, Genoa 16147 Italy. Tel: +39 01056363270; Fax: +39 010.3779798; E-mail: andrearossi@gaslini.org

Funding Information

This work was supported by funds from "Ricerca Corrente sui Disordini Neurologici e Muscolari (Linea 5)" of the Italian Ministry of Health.

Received: 18 May 2021; Revised: 9 August 2021; Accepted: 11 August 2021

Annals of Clinical and Translational Neurology 2021; 8(10): 2004–2012

doi: 10.1002/acn3.51448

Abstract

Data on fetal MRI in L1 syndrome are scarce with relevant implications for parental counseling and surgical planning. We identified two fetal MR imaging patterns in 10 fetuses harboring *L1CAM* mutations: the first, observed in 9 fetuses was characterized by callosal anomalies, diencephalosynapsis, and a distinct brainstem malformation with diencephalic–mesencephalic junction dysplasia and brainstem kinking. Cerebellar vermis hypoplasia, aqueductal stenosis, obstructive hydrocephalus, and pontine hypoplasia were variably associated. The second pattern observed in one fetus was characterized by callosal dysgenesis, reduced white matter, and pontine hypoplasia. The identification of these features should alert clinicians to offer a prenatal *L1CAM* testing.

Introduction

L1CAM encodes for the L1 cell adhesion molecule, a membrane glycoprotein mediating cell-to-cell adhesion at the cell surface.¹ Pathogenic variants of *L1CAM* (MIM *308840) are responsible for a spectrum of X-linked disorders collectively known as L1 syndrome, including X-linked hydrocephalus with aqueductal stenosis (HSAS), mental retardation, aphasia, shuffling gait, adducted thumbs (MASA) syndrome, and isolated partial corpus callosum agenesis (CCA).¹ Postnatal imaging features include obstructive hydrocephalus, CCA, enlarged quadrigeminal plate, interthalamic adhesion hypertrophy, and vermian hypoplasia.² Moreover, data on fetal MRI are scarce with relevant implications for counseling and surgical planning.^{3–6} In particular, little information is available on the prenatal appearance of midbrain–hindbrain structures in this condition.

Diencephalic–mesencephalic junction (DMJ) dysplasia (DMJD) is a rare midbrain–hindbrain malformation characterized by a poorly defined junction between the diencephalon and mesencephalon, variably associated with other brain malformations, including CCA and ventricular dilation.⁷ We previously identified two DMJD patterns characterized by abnormal cleavage between the midbrain and hypothalamus in the axial plane (type A-DMJD) and fusion between the midbrain and thalamus in the sagittal plane (type B-DMJD).⁸ The former includes the “butterfly-like” pattern, originally reported by Zaki et al. and recently associated with biallelic pathogenic variants in *PCDH12*.⁹ Of note, a subset of type A-DMJD is associated with obstructive ventriculomegaly and can be recognized by fetal MRI during the second-third trimester of pregnancy.¹⁰ We previously suggested that these DMJD cases were potentially linked to *L1CAM* mutations, yet no genetic testing was performed at that time.¹⁰ Recently, the largest series of fetal DMJD has been reported, unveiling the contribution of *L1CAM* mutations in four out of seven subjects tested for this gene.¹¹ Interestingly, different patterns of DMJD were associated with *L1CAM* variants, including a new subtype overlapping with type-B DMJD, characterized by complete thalamic–midbrain fusion on the sagittal plane. Of note, data on additional brainstem anomalies were only provided in one fetus.¹¹

Here, we describe 10 fetal cases harboring 9 *L1CAM* pathogenic variants, providing evidence that deleterious variants in this gene may cause a recognizable brainstem malformation variably associated with diencephalosynapsis, ventriculomegaly, and CCA.

Methods

In this multicenter retrospective study, approved by the Liguria’s Regional Ethical Board, we included 10 male

fetuses from 9 distinct families with genetically confirmed L1 syndrome who underwent fetal brain MRI in six pediatric hospitals over 10 years (2010–2020). Written informed consent was obtained from participants or legal representatives.

Clinical data were retrieved from electronic charts. Fetal MRI studies were performed on 1.5T or 3.0T scanners with a phased-array abdominal or cardiac coil after a neurosonography study. All studies included 3-mm-thick single-shot fast spin-echo multiplanar T2-weighted images. Post-mortem MRI studies were performed on 1.5T or 3.0T scanners with dedicated protocols as previously reported.¹² MRI examinations were reviewed in consensus by pediatric neuroradiologists. Midbrain–hindbrain malformations were classified according to the 2009 Barkovich classification,¹³ while DMJD was defined as type A or B based on previous criteria.⁸ Biometry of posterior cranial fossa structures was compared with reference data.^{14,15} Ventriculomegaly was classified as mild (10–12mm), moderate (12–15 mm), or severe (>15 mm).

Available histopathological findings were reviewed by experienced pathologists. Genomic DNA extracted from fetal tissues was screened for *L1CAM* mutations by targeted Sanger or Next-generation sequencing. All *L1CAM* variants were reported according to the NM_000425.4 transcript and classified according to the American College of Medical Genetics and Genomics criteria (ACMG).

Results

Clinical, neuroimaging, and genetic characteristics are detailed in Tables 1 and 2, and in Table S1. The average maternal age was 33.3 years (range 23–37 years). A positive family history was present in 7/10 (70%) cases. The median gestational age at MRI was 21.5 weeks (range 20–32). Adducted thumb/clenched hands were noted in 8/10 (80%) cases. Ventriculomegaly and adducted thumbs detected by the prenatal US in the majority of fetuses were the main reason for requesting fetal MRI.

At fetal MRI, two distinct imaging phenotypes were detected (Figures 1 and 2, Fig. S1). The first, observed in nine fetuses, was characterized by callosal anomalies, reduced opercularization, diencephalosynapsis, brainstem kinking, and features of both DMJD type A and B. On axial images, the midbrain showed an enlarged dorsoventral axis, fusion with the hypothalamus, and a ventral cleft (“butterfly sign”). On sagittal images, the enlarged massa intermedia was caudally displaced and apparently fused with the midbrain. Additional features included obstructive hydrocephalus (7/9), small vermis (8/9), aqueductal stenosis (7/9), and short pons (4/9). In the other phenotype, observed in one fetus, callosal dysgenesis was

Table 1. Clinical, neuroimaging and genetic findings of subjects with L1CAM variants.

Subject	#1	#2	#3	#4	#5	#6	#7	#8	#9	#10
Ethnicity	Caucasian Italian	Caucasian Italian	Caucasian Italian	Caucasian Italian	Caucasian Australian	Iranian	Iranian	Caucasian British	Jewish Ashkenazi	Chinese Asian
FH of fetuses/males with hydrocephalus and DD	+	+	-	+	+	+	+	+	+	-
Fetal MRI GW	21	20	21	20	22	20	26	22	22	33
CCA	Marked hypoplasia Severe	Partial agenesis Severe	Marked hypoplasia Severe	Marked hypoplasia Moderate-severe	Marked hypoplasia Severe	Marked hypoplasia Severe	Marked hypoplasia Severe	Complete agenesis	Complete agenesis	Partial agenesis
VM ¹										Unilateral severe
RO	+	+	+	+	+	+	+	+	+	Dysgyria
Type A DMJD	+	+	+	+	+	+	+	+	+	-
Type B DMJD	+	+	+	+	+	+	+	+	+	-
Diencephalo-synapsis	+	+	+	+	+	+	+	+	+	-
BK	+	+	+	+	+	+	+	+	+	-
AS	-	+	+	+	+	+	+	-	+	-
Pontine hypoplasia	-	-	+	+	+	+	+	-	-	+
Vermian hypoplasia	+	-	+	+	+	+	-	+	+	+
CH hypoplasia	-	-	+	-	-	-	-	-	-	-
Adducted thumb	+	+	+	-	+	+	+	-	+	+
Outcome	TOP	TOP	TOP	TOP	Fetal demise	TOP	TOP	TOP	TOP	MASA syndrome
Postnatal or postmortem brain MRI	-	-	Post-mortem MRI: thin and upward displaced CC, AS, severe VM, thinning of the posterior cerebral parenchyma, reduced pontine CCD	-	Post-mortem MRI: severe bilateral VM, AS, severe VM, dysgyria, BK	-	-	-	-	MRI at 2 years: CC hypodysgenesis, VM, reduced VM volume, pontine hypoplasia, dysgyria

(Continued)

Table 1 Continued.

Subject	#1	#2	#3	#4	#5	#6	#7	#8	#9	#10
Histopathological findings	Mild craniofacial dysmorphism, clenched hands, VM, marked CC hypoplasia, fused thalami, dysgyria	Mild craniofacial dysmorphism, adducted thumbs, VM, patent cerebral aqueduct, agenesis of the pyramidal tracts, normal cortical lamination	Mild craniofacial dysmorphism, clenched hands, VM, patent cerebral aqueduct, cerebral agenesis of the pyramidal tracts, normal cortical thinning, abnormal small cortical sulci	NA	VM, AS, normal cortical gyration, small medullary pyramids, cerebellar neuronal heterotopias	–	–	Mild craniofacial dysmorphism, CC agenesis, normal gyral pattern, normal cerebellum	–	–
L1CAM variants (NML_000425.4)	Exons 1–6 deletion	c.2092G>A, p.(Gly698Arg)	c.1849delC p.(Arg617 Glyfs*10)	c.1672C>T p.(Arg558*)	c.551G>A p.(Arg184Gln) Glyfs*112	c.2215delC p.(Arg739 Glyfs*112)	c.2215delC p.(Arg739 Glyfs*112)	c.3201del p.(Tyr1067*)	c.791G>A p.(Cys264Tyr)	c.2260T>A p.(Trp754Arg)

ACMG, American College of Medical Genetics; AA, amino acid; APD, antero-posterior diameter; AS, aqueductal stenosis; BK, brainstem kinking; CC, corpus callosum; CCA, corpus callosum anomaly; CCA, corpus callosum anomaly; CH, cerebellar hemispheres; CNS, central nervous system; CS, cesarean section; CSP, cavum septum pellucidum; DD, developmental delay; DMJD, diencephalic mesencephalic junction dysplasia; FM, family history; GW, gestational week; NA, not available; NMD, nonsense-mediated mRNA decay; FFPE, Formalin-fixed paraffin-embedded; RO, reduced opercularization; TD, transverse diameter; TOP, termination of pregnancy; US, ultrasound; VM, Ventriculomegaly; VP, ventriculoperitoneal; WES, whole-exome sequencing; WM, white matter.

¹Involving only the lateral ventricles.

Table 2. Main neuroimaging features of the two patterns associated with L1 syndrome based on the present series and the literature.

	L1 Phenotype – type 1	L1 Phenotype – type 2
Supratentorial anomalies		
Corpus callosum	Hypoplasia, partial or complete agenesis	Hypoplasia, partial or complete agenesis
Ventricular system	Moderate to severe dilatation usually symmetric reduced or increased III ventricle	Mild to moderate dilatation usually asymmetric normal III ventricle size
Cortical development	Reduced opercularization Neuronal migration disorders (rare)	Insular dysgyria Neuronal migration disorders (rare)
White matter	Diffusely reduced volume	Reduced volume, mainly in posterior regions
Thalami	Diencephalosynapsis	Normal or absent interthalamic mass
Diencephalic-mesencephalic junction	DMJD type A and B	Normal
Infratentorial anomalies		
Cerebral aqueduct	Aqueductal stenosis (variably present)	Patent
Brainstem	Brainstem kinking Mild to moderate pontine hypoplasia (variably present)	Mild pontine hypoplasia (variably present)
Cerebellum	Vermian hypoplasia (variably present) Cerebellar hemisphere hypoplasia (rare)	Vermian hypoplasia (variably present) Normal cerebellar hemispheres

DMJD, diencephalic-mesencephalic junction dysplasia.

associated with asymmetric ventriculomegaly, reduced white matter volume, dysgyria, and pontine hypoplasia.

In eight cases, parents decided on the termination of pregnancy. One subject died at birth due to perinatal complications: a cephalocentesis was performed to enable delivery by cesarean section, resulting in severe bradycardia and fetal demise. The only surviving subject is a 10-year-old boy with MASA syndrome (Figure 2 and Data S1). Post-mortem MRI and autopsy were performed in 2/8 and 5/8 cases, respectively, and confirmed the features identified at fetal MRI (Figure 1D–F, Fig. S2).

We identified 9 pathogenic or likely pathogenic *L1CAM* variants in 10 fetuses (Table 1). All variants are absent from the gnomAD database (<https://gnomad.broadinstitute.org>) and 5 are *novel*. The nonsense and frameshift variants were predicted to result in premature truncation of the transcript, likely leading to nonsense-mediated mRNA decay. The missense variants affected highly conserved residues and were predicted to have a deleterious effect according to ACMG criteria.

Discussion

We describe the neuroimaging features of the largest cohort of fetuses harboring *L1CAM* mutations, unraveling two distinct patterns that mainly differ for the brainstem appearance (Table 2). In addition to callosal anomalies and/or hydrocephalus, the majority of fetuses presented a peculiar brainstem malformation characterized by features of both DMJD type A and B, brainstem kinking, and a variable combination of aqueductal stenosis, short pons, and small vermis. In particular, on axial

images, the midbrain was fused with the hypothalamus and showed a ventral cleft leading to the so-called “butterfly-like” appearance of type A-DMJD.^{7,10,16} On sagittal images, the interthalamic mass was enlarged and caudally displaced leading to partial third ventricle atresia, as described in diencephalosynapsis,¹⁷ in apparent continuity with the midbrain, as described in type B-DMJD. These features were confirmed on post-mortem MRI. Remarkably, thalamic–mesencephalic fusion on sagittal planes should be reassessed after birth, since this might be over-estimated on fetal MRI due to its limited spatial resolution, as shown by Lawrence et al.¹¹ It is noteworthy that pathological data of roughly 100 fetal cases of genetically confirmed L1 syndrome have been reported yet none of them described in detail the DMJ.¹⁸ This is likely because the vast majority of these cases were identified prior to the recognition of DMJD as a distinct neuroradiological sign, thereby suggesting that the occurrence of DMJD might be underestimated in L1 fetuses. Of note, the combination of hydrocephalus, CCA, diencephalosynapsis, DMJD, brainstem kinking, and early anteroposterior/dorsoventral patterning brainstem defects might facilitate the prenatal identification of *L1CAM* mutations, thus helping with timely prenatal counseling. Moreover, this might have relevant implications in the surgical management of congenital hydrocephalus, since DMJD and diencephalosynapsis obliterate the floor of the third ventricle preventing endoscopic third ventriculostomy procedures.¹⁹ Finally, brainstem evaluation on fetal MRI is fundamental in cases of presumed aqueduct stenosis, because brainstem malformations are largely undiagnosed or undiagnosable

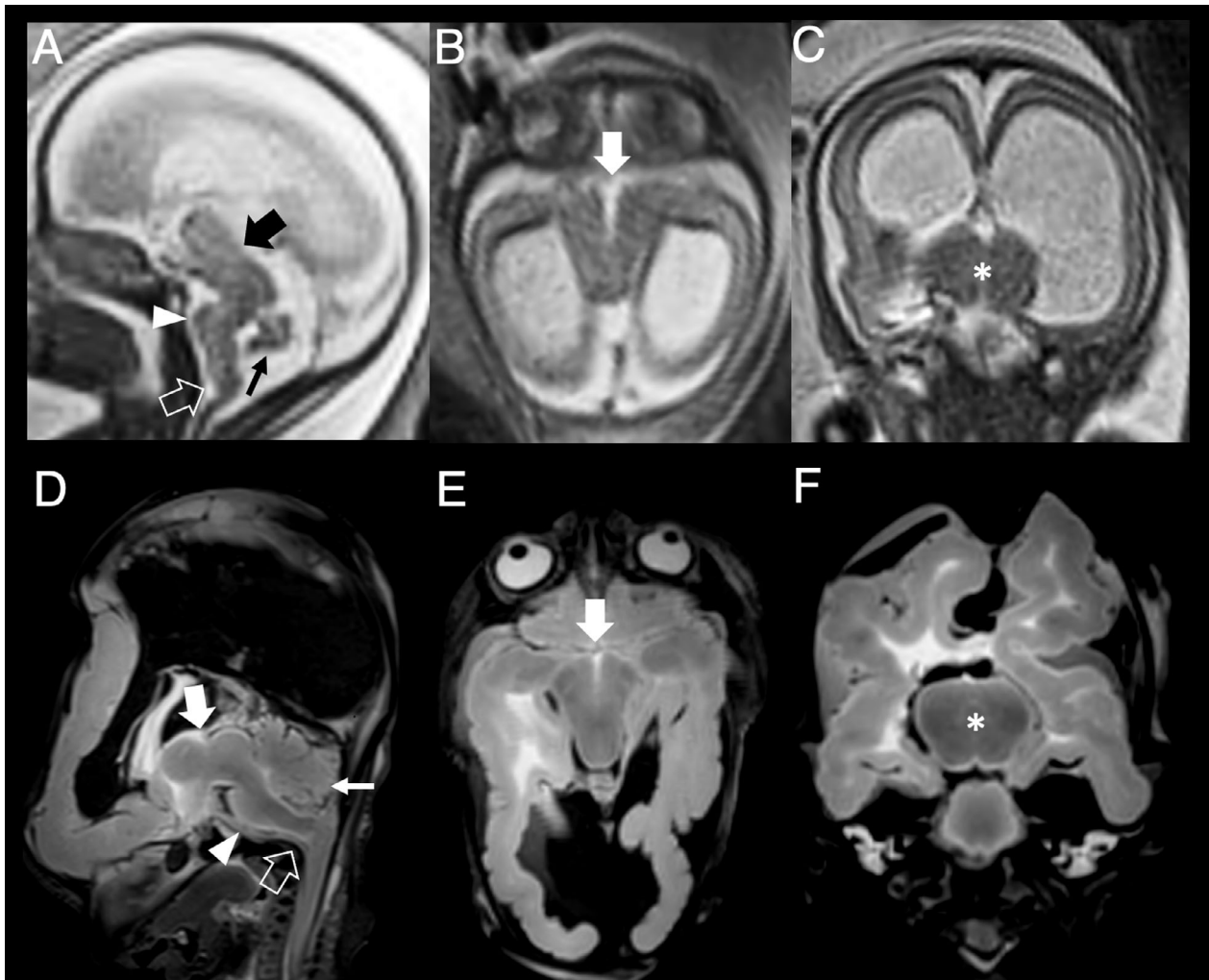


Figure 1. Fetal brain MRI (A–C) and post-mortem MRI (D–F) in a 22-week-old fetus. Sagittal (A, D), axial (B, E), and coronal (C, F) T2-weighted images show the most frequent neuroimaging pattern, characterized by obstructive hydrocephalus, marked thinning of the corpus callosum, diencephalosynapsis (asterisks), features of DMJD type B on the sagittal plane (thick arrows, A, D), features of DMJD type A with typical butterfly appearance of the midbrain on the axial plane (thick arrows, B, E), brainstem kinking (empty arrows), pontine hypoplasia (arrowheads), and small vermis (thin arrows).

with prenatal ultrasound but impact significantly on neurodevelopmental outcome.

The L1 cell adhesion molecule plays pivotal roles in neuronal adhesion, neuronal migration, axonal growth and pathfinding, and in the development of the ventricular system and cerebellum.²⁰ However, its contribution to the formation and positioning of the DMJ remains unclear. To date, several molecules including the Paired box 2 and 6 (*Pax2*, *Pax6*), *Engrailed-1* (*En1*), and *Fibroblast growth factor 8* (*Fgf8*) have been claimed to play a crucial function in the DMJ development.^{21,22} *PCDH12*, originally described to mediate cell adhesion in endothelial cells, was recently shown to promote

neurite outgrowth and its deficiency perturbed the correct DMJ development in patients carrying biallelic mutations.⁹ Likewise, other cell adhesion molecules involved in neuronal migration and axon guidance may contribute to the mid-hindbrain development. In mice, *L1CAM* is expressed on tangential fibers in the ventral midbrain where it modulates axonal growth via trans-heterophilic interaction with *PTPRZ1* (Protein Tyrosine Phosphatase, Receptor Type Z, polypeptide 1) and *ALCAM* (Activated Leukocyte Cell Adhesion Molecule) that are expressed in murine midbrain dopamine (mDA) neurons.^{23,24} Interestingly, in *L1CAM* knockout mice, mDA neurons appear to be abnormally positioned,²⁵

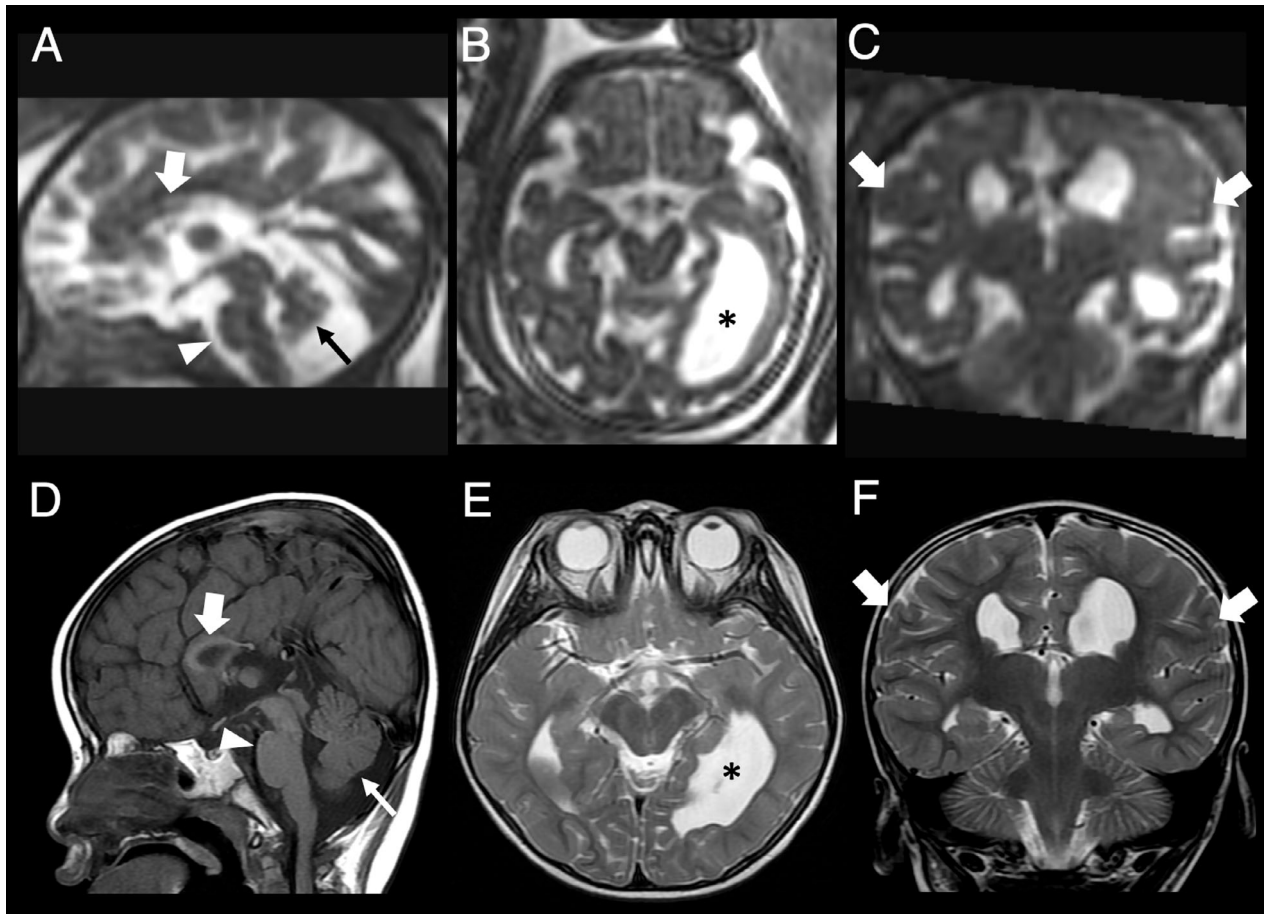


Figure 2. Fetal brain MRI at 32 gestational weeks (A–C) and postnatal MRI performed at 2 years of age (D–F) of subject #10. Sagittal (A, D), axial (B, E), and coronal (C, F) T2-weighted and T1-weighted images reveal the other neuroimaging pattern, characterized by marked white matter volume reduction with asymmetric ventriculomegaly (asterisks, B, E), bilateral dysgyria (thick arrows, C, F), dysgenesis of the corpus callosum (thick arrows, A, D), normal DMJ, mild pontine hypoplasia (arrowheads, A, D), and small vermis (thin arrows, A, D).

underscoring a pivotal role of *L1CAM* in migration and pathfinding also for midbrain neurons with consequent possible involvement in DMJ formation.

The second phenotype, identified in one fetus presenting after birth with a MASA syndrome, was characterized by callosal dysgenesis, reduced white matter volume, and pontine hypoplasia. Interestingly, these features have been recently described in five subjects harboring *L1CAM* mutations presenting with mild intellectual disability, even in the absence of adducted thumbs.²⁶ Moreover, four additional subjects with MASA syndrome reported in the literature presented similar brain abnormalities.^{2,27–29} Considered the rarity of L1 disorders and the fact that subjects without obstructive hydrocephalus may not immediately be recognized as potential L1 mutation cases, we submit that this L1 phenotype may remain largely underdiagnosed. Future studies on larger cohorts are awaited to shed light on this intriguing hypothesis.

Finally, although model mice with different sites of *L1CAM* mutation have been studied, the pathogenetic mechanisms of ventricular dilatation in L1 syndrome remain unsolved. Considering that *L1CAM* is involved in axonal growth and fasciculation,³⁰ several hypotheses have been formulated, including: i) the hypoplasia of the white matter secondary to poor neuronal connections, ii) the increase in brain compliance due to the loss of L1-mediated adhesion between axons, leading to an increase in ventricle size even with normal cerebrospinal fluid pressure, and iii) the alteration of the shape and caliber of the cerebral aqueduct leading to obstructive hydrocephalus.^{31–33} An alternative explanation for the obstructive hydrocephalus observed in fetuses without aqueductal stenosis presenting with the first L1 phenotype could be related to the presence of diencephalosynapsis causing partial or complete III ventricle atresia.¹⁷ Conversely, we speculate that the asymmetric ventriculomegaly observed

in the second L1 phenotype might be better explained by primary hypoplasia of the white matter and/or by an increase in brain compliance.

In summary, in the majority of fetuses, we identified a peculiar diencephalic and midbrain–hindbrain malformation that especially when associated with hydrocephalus and CCA should alert clinicians to offer a prenatal *L1CAM* testing. The prenatal diagnosis of L1 disorder would be extremely important to guide parents through the challenging decision-making process regarding the option of a therapeutic abortion. Further genetic studies extending the *L1CAM* genetic analysis to male fetuses with callosal anomalies, reduced white matter volume, and pontine hypoplasia are needed to understand the real prevalence of rarer L1 imaging phenotypes.

ACKNOWLEDGMENTS

This work was supported by funds from “Ricerca Corrente sui Disordini Neurologici e Muscolari (Linea 5)” of the Italian Ministry of Health.

CONFLICT OF INTEREST

LM consults for Mendelian Ltd, a rare disease digital health company. All other authors report no financial disclosure/conflict of interest concerning the research related to the manuscript.

AUTHORS' CONTRIBUTION

Conception and Design of the study, Acquisition and analysis of data, and Drafting a significant portion of the manuscript or figures: Andrea Accogli, Stacy Goergen, Giana Izzo, Kshitij Mankad, Karina Kraiden Haratz, Cecilia Parazzini, Michael Fahey, Lara Menzies, Julia Baptista, Lucia Carpineta, Domenico Tortora, Ezio Fulcheri, Valerio Gaetano Vellone, Dario Paladini, Luigina Spaccini, Valentina Toto, Claire Trayers, Liat Ben Sira, Adi Reches, Gustavo Malinger, Vincenzo Salpietro, Patrizia De Marco, Myriam Srour, Federico Zara, Valeria Capra, Andrea Rossi, Mariasavina Severino.

REFERENCES

1. Stumpel C, Vos YJ. L1 Syndrome. 2004 Apr 28 [Updated 2021 Jan 7]. In: Adam MP, Ardinger HH, Pagon RA, Wallace SE, eds. GeneReviews® [Internet]. Seattle, WA: University of Washington, 1993–2021. Accessed March 1, 2021. <https://www.ncbi.nlm.nih.gov/books/NBK1484/>.
2. Kanemura Y, Okamoto N, Sakamoto H, Shofuda T, Kamiguchi H, Yamasaki M. Molecular mechanisms and neuroimaging criteria for severe L1 syndrome with X-linked hydrocephalus. *J Neurosurg*. 2006;105:403-412.
3. Guo D, Shi Y, Jian W, et al. A novel nonsense mutation in the *L1CAM* gene responsible for X-linked congenital hydrocephalus. *J Gene Med*. 2020;22:e3180.
4. Stowe RC, Lyons-Warren AM, Emrick L. Clinical reasoning: ventriculomegaly detected on 20-week anatomic fetal ultrasound. *Neurology*. 2018;91:e1265-e1268. doi: <https://doi.org/10.1212/WNL.0000000000006247>
5. Ochando I, Vidal V, Gascón J, Ación M, Urbano A, Rueda J. Prenatal diagnosis of X-linked hydrocephalus in a family with a novel mutation in *L1CAM* gene. *J Obstet Gynaecol*. 2016;36:403-405.
6. Serikawa T, Nishiyama K, Tohyama J, et al. Prenatal molecular diagnosis of X-linked hydrocephalus via a silent C924T mutation in the *L1CAM* gene. *Congenit Anom*. 2014;54:243-245.
7. Zaki MS, Saleem SN, Dobyns WB, et al. Diencephalic-mesencephalic junction dysplasia: a novel recessive brain malformation. *Brain*. 2012;135:2416-2427. doi: <https://doi.org/10.1093/brain/aws162>
8. Severino M, Tortora D, Pistorio A, et al. Expanding the spectrum of congenital anomalies of the diencephalic-mesencephalic junction. *Neuroradiology*. 2016;58:33-44. doi: <https://doi.org/10.1007/s00234-015-1601-x>
9. Guemez-Gamboa A, Çağlayan AO, Stanley V, et al. Loss of protocadherin-12 leads to diencephalic-mesencephalic junction dysplasia syndrome. *Ann Neurol*. 2018;84:638-647.
10. Severino M, Righini A, Tortora D, et al. MR imaging diagnosis of diencephalic-mesencephalic junction dysplasia in fetuses with developmental ventriculomegaly. *Am J Neuroradiol*. 2017;38:1643-1646.
11. Lawrence AK, Whitehead MT, Kruszka P, et al. Prenatal diagnosis of diencephalic-mesencephalic junction dysplasia: fetal magnetic resonance imaging phenotypes, genetic diagnoses, and outcomes. *Prenat Diagn*. 2021;41(6):778-790. doi: <https://doi.org/10.1002/pd.5909>
12. Scola E, Conte G, Palumbo G, et al. High resolution post-mortem MRI of non-fixed in situ foetal brain in the second trimester of gestation: normal foetal brain development. *Eur Radiol*. 2018;28:363-371.
13. Barkovich AJ, Millen KJ, Dobyns WB. A developmental and genetic classification for midbrain-hindbrain malformations. *Brain*. 2009;132:3199-3230. doi: <https://doi.org/10.1093/brain/awp247>
14. Tilea B, Alberti C, Adamsbaum C, et al. Cerebral biometry in fetal magnetic resonance imaging: new reference data. *Ultrasound Obstet Gynecol*. 2009;33:173-181.
15. Conte G, Milani S, Palumbo G, et al. Prenatal brain MR imaging: reference linear biometric centiles between 20 and 24 gestational weeks. *Am J Neuroradiol*. 2018;39:963-967.
16. Severino M, Huisman TAGM. Posterior fossa malformations. *Neuroimaging Clin N Am*. 2019;29:367-383. doi: <https://doi.org/10.1016/j.nic.2019.03.008>
17. Cagneaux M, Vasiljevic A, Massoud M, et al. Severe second-trimester obstructive ventriculomegaly related to

- disorders of diencephalic, mesencephalic and rhombencephalic differentiation. *Ultrasound Obstet Gynecol.* 2013;42:596-602.
18. Adle-Biassette H, Saugier-Verber P, Fallet-Bianco C, et al. Neuropathological review of 138 cases genetically tested for X-linked hydrocephalus: evidence for closely related clinical entities of unknown molecular bases. *Acta Neuropathol.* 2013;126:427-442.
 19. Furtado LM, da Costa Val Filho JA, Holliday JB, et al. Endoscopic third ventriculostomy in patients with myelomeningocele after shunt failure. *Childs Nerv Syst.* 2020;36:3047-3052.
 20. Itoh K, Fushiki S. The role of L1cam in murine corticogenesis, and the pathogenesis of hydrocephalus. *Pathol Int.* 2015;65:58-66.
 21. Nakamura H, Watanabe Y. Isthmus organizer and regionalization of the mesencephalon and metencephalon. *Int J Dev Biol.* 2005;49:231-235.
 22. Scholpp S, Lohs C, Brand M. Engrailed and Fgf8 act synergistically to maintain the boundary between diencephalon and mesencephalon. *Development.* 2003;130:4881-4893. doi:<https://doi.org/10.1242/dev.00683>
 23. Ohyama K, Kawano H, Asou H, et al. Coordinate expression of L1 and 6B4 proteoglycan/phosphacan is correlated with the migration of mesencephalic dopaminergic neurons in mice. *Dev Brain Res.* 1998;107:219-226.
 24. Bye CR, Rytova V, Alsanie WF, Parish CL, Thompson LH. Axonal growth of midbrain dopamine neurons is modulated by the cell adhesion molecule ALCAM through -heterophilic interactions with L1cam, Chl1, and semaphorins. *J Neurosci.* 2019;39:6656-6667.
 25. Demyanenko GP, Shibata Y, Maness PF. Altered distribution of dopaminergic neurons in the brain of L1 null mice. *Dev Brain Res.* 2001;126:21-30.
 26. Bousquet I, Bozon M, Castellani V, et al. X-linked partial corpus callosum agenesis with mild intellectual disability: identification of a novel L1CAM pathogenic variant. *Neurogenetics.* 2021;22(1):43-51. doi:<https://doi.org/10.1007/s10048-020-00629-y>
 27. Kanemura Y, Takuma Y, Kamiguchi H, Yamasaki M. First case of L1CAM gene mutation identified in MASA syndrome in Asia. *Congenit Anom.* 2005;45:67-69. doi:<https://doi.org/10.1111/j.1741-4520.2005.00067.x>
 28. Basel-Vanagaite L, Straussberg R, Friez MJ, et al. Expanding the phenotypic spectrum of L1CAM-associated disease. *Clin Genet.* 2006;69:414-419. doi:<https://doi.org/10.1111/j.1399-0004.2006.00607.x>
 29. Otter M, Wevers M, Pisters M, et al. A novel mutation in L1CAM causes a mild form of L1 syndrome: a case report. *Clin Case Rep.* 2017;15:1213-1217. doi:<https://doi.org/10.1002/ccr3.1038>
 30. Wiencken-Barger AE, Mavity-Hudson J, Bartsch U, Schachner M, Casagrande VA. The role of L1 in axon pathfinding and fasciculation. *Cereb Cortex.* 2004;14:121-131. doi:<https://doi.org/10.1093/cercor/bhg110>
 31. Dahme M, Bartsch U, Martini R, Anliker B, Schachner M, Mantei N. Disruption of the mouse L1 gene leads to malformations of the nervous system. *Nat Genet.* 1997;17:346-349. doi:<https://doi.org/10.1038/ng1197-346>
 32. Fransen E, D'Hooge R, Van Camp G, et al. L1 knockout mice show dilated ventricles, vermis hypoplasia and impaired exploration patterns. *Hum Mol Genet.* 1998;7:999-1009. doi:<https://doi.org/10.1093/hmg/7.6.999>
 33. Rolf B, Kutsche M, Bartsch U. Severe hydrocephalus in L1-deficient mice. *Brain Res.* 2001;891:247-252. doi:[https://doi.org/10.1016/s0006-8993\(00\)03219-4](https://doi.org/10.1016/s0006-8993(00)03219-4)

Supporting Information

Additional supporting information may be found online in the Supporting Information section at the end of the article.

Figure S1. Fetal MRI findings in L1 syndrome. Fetal MRI of a control fetus at 21 gestational weeks (A) and of fetuses #1–9 harboring *L1CAM* variants (B–J). B–J) Sagittal (top row), axial (middle row), coronal (bottom row) T2-weighted images show marked thinning or agenesis of the corpus callosum, diencephalosynapsis, features of both DMJD type A and B, and brainstem kinking in all fetuses. Aqueductal stenosis is present in fetuses #2–7 and #9 (arrows), while pontine hypoplasia is observed in fetuses #3–7 (arrowheads), and small vermis in fetuses #1, #3–6, #8, #9 (thick arrows).

Figure S2. Macroscopic appearance in the fixed brain of the diencephalic–mesencephalic region in fetus #1. A, B) Coronal slices through the fixed brain show ventriculomegaly with thinning of the cerebral parenchyma, agenesis of the corpus callosum (arrowhead), fusion of the thalami with atresia of the third ventricle consistent with diencephalosynapsis (empty arrows), and fusion between the midbrain and thalamus (thick arrows).

Table S1. Clinical, neuroimaging and genetic findings of subjects with *L1CAM* variants.

Data S1. Supplemental case report.